

Synthesis of Gold Nanorods & CdSe Quantum Dots

Felix Syn CID: 02193782

Undergraduate Laboratory for MBE Students, Imperial College London

ABSTRACT: This paper explores the synthesis of Gold Nanorods(AuNRs) and Cadmium Selenide(CdSe) Quantum Dots (QDs). Batches of AuNRs were synthesised to compare the effects of different surfactant types that differ in chain length while in QD synthesis, we injected Cd and Se precursor solutions into a growth solution to observe the effect oleylamine has on the appearance of QD solutions under ambient and UV light. Overall results demonstrate that longer chain surfactants help to increase the aspect ratio of AuNRs due to greater steric hindrance. Oleylamine narrows the emission spectrum peaks in QD synthesis due to reduced trap state emission.

INTRODUCTION: Nanoparticles are particles with at least one dimension on the order of 10^{-9} m (1nm). Their small size causes surface properties to dominate over bulk properties which leads to some interesting effects. Surface properties have been utilised throughout history for aesthetic purposes and have gained popularity due to their potential medical uses. Synthesising gold (Au) nanorods and quantum dots have allowed us to study their quantum properties such as surface plasmon resonance (SPR) and quantum size effects. This is where nanoparticles exhibit a different colour due to the interaction of electrons of surface atoms and incident light. This paper explores the synthesis of Au Nanorods and Quantum Dots and tries to explain the results we attain.

METHODS: We first observed the effects of 2 different surfactants (CTAB & C14TAB) during Gold Nanorods (AuNR) synthesis. 4 empty, labelled test tubes (B1, B2, B3, B4) were prepared and filled according to the table below:

	B1	B2	B3	B4
CTAB(C16TAB)	4.75ml	2.50ml	-	-
C14TAB	-	-	4.75ml	2.50ml
Distilled Water	0.25ml	2.50ml	0.25ml	2.50ml

Micropipette 0.2ml of 0.01M $\text{HAuCl}_4 \cdot 3\text{H}_2\text{O}$ then 0.03ml of 0.01M AgNO_3 to each tube. Mix by inverting the tubes. The colour should be slightly brown. Leave in water bath (25-30°C). Add 0.032ml Ascorbic Acid (AA) to each tube, mix by inverting the tubes and place back into the water bath. Add 0.01ml Au seed solution to each tube, mix by inverting tube and place back in the water bath. Start stopwatch upon

addition. Record absorbances at 530nm, 700nm and 800nm every 5 minutes for 15 minutes, then every 15 minutes for an hour. The timestamps for recording are 5 min, 10 min, 15 min, 30 min, 45 min and 60 min.

Quantum Dots synthesis was carried out by pipetting 1ml of a Cd precursor solution and a Se precursor solution into a growth solution. Procedure 1 growth solution was 10ml octadecene+0.67ml oleylamine and Procedure 2 growth solution only had 10ml octadecene. Cd precursor solution contained Cadmium Acetate($\text{Cd}(\text{Ac})_2$), oleic acid ($\text{R}-\text{COOH}$) and octadecene. Se precursor solution contained dissolved Se powder in trioctylphosphene(TOP). Heat the Cd precursor solution to about 130C and the Growth Solution to 165C. When ready, extract 1ml of Se precursor solution and 1ml of Cd precursor solution with separate syringes. Both precursor solutions were added to the heated Growth Solution simultaneously and a timer was set. 1ml of the growth solution was extracted at the times: 15sec, 30sec, 1min, 1.5min, 2min, 2.5min, 3.5min, 4.5min, 5.5min, 6.5min and placed in separate vials (1-10 respectively) and cooled down in an ice bath to room temperature. The cooled solution samples were viewed under ambient light and UV light. Photos were taken. The solutions were then sent for UV-Vis spectroscopy to attain emission and absorption spectrographs.

RESULTS:

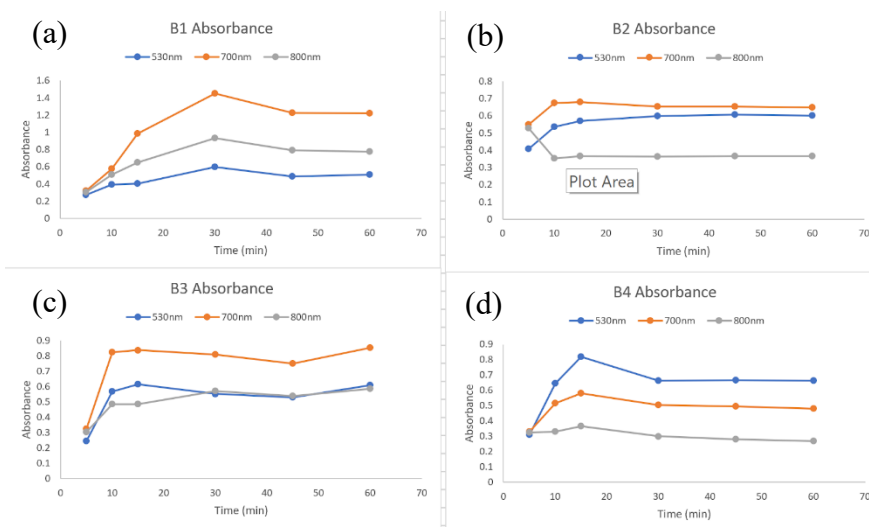


Figure 1: Absorbance against Time graphs for B1(a), B2 (b), B3 (c) and B4 (d) at each wavelength: 530nm (Blue), 700nm (Orange), 800nm (Grey)

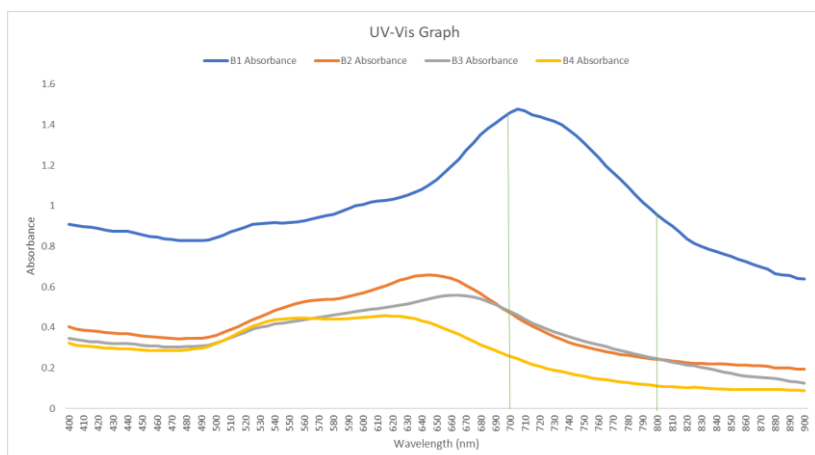



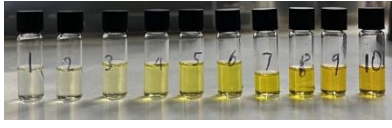

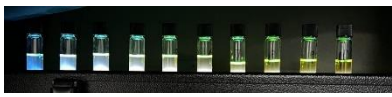
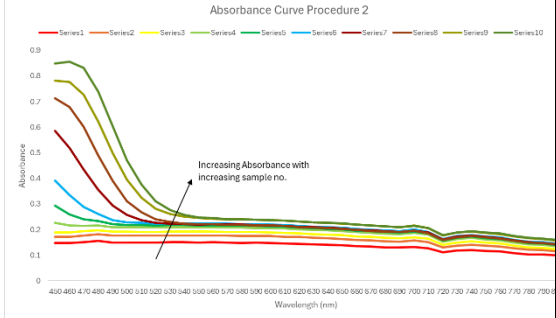
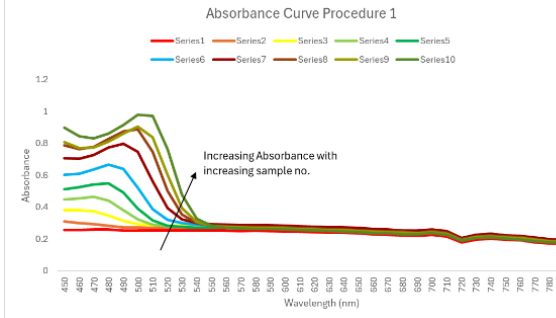
Figure 2: A UV-Vis Spectrograph for B1 (Blue), B2(Orange), B3(Grey) and B4(Yellow) from 400nm to 900nm. 5nm interval between each absorbance reading.

For AuNR synthesis, Figure 1 suggests that for B1 and B4, the absorbances over time at each wavelength 530nm, 700nm and 800nm initially increases until a peak. followed by a small decrease that leads into a plateau after some time. B3 appears to follow this trend as well except at 800nm where absorbance increases until a plateau is reached. An anomaly occurs between the first and second reading at 800nm for B2. This could be due to placing the cuvette in a different orientation in the spectrometer initially compared to the rest of the measurements. This would be a point for improvement in the future since a different cuvette orientation can lead to a significant error in absorbance readings.

Figure 2 indicates that the overall absorbance for B1 at each wavelength is greater compared to the other samples. The peak wavelength where absorbance is maximum is also the highest for B1. The peak wavelengths for samples B1, B2, B3 and B4 were 705nm, 645nm, 665nm and 615nm respectively which corresponds to an Aspect Ratio (AR) of 3.33, 2.69, 2.91 and 2.37 respectively.

Brioude et al. proposed an equation relating nanorod Aspect Ratio (length/width) to longitudinal plasmon resonance wavelength (2005, p. 13140): $\lambda = 93.72(AR) + 392.6$. This relation was used to calculate the AR in the table above. We observe that B1 has the largest aspect ratio (longest AuNRs) followed by B3, B2 then B4. We can immediately see that AuNRs made with CTAB (B1 and B2) produced longer nanorods than those made with C14TAB (B3 and B4 respectively).

For CdSe QD synthesis, the reaction mixture was initially transparent in ambient light. Reacted sample solutions in both experiments had colours from transparent to different shades of yellow. It was apparent that the samples extracted at a longer time (vials 5 to 10) were more yellow than those extracted at an earlier time. Under UV light however, the solutions fluoresce in a range of colours from blue to bright yellow(from 1 to 10). It was noted that the growth solution temperature only reached 150C at maximum heating due to the inefficiencies of the heater, which is lower than the desired 165C. As such, the solution colours may differ from ideal results under ambient and UV light.

	Without Oleylamine (Procedure 2)	With Oleylamine (Procedure 1)
Ambient Light		
UV Light		
Absorption Spectra	 <p>Absorption Curve Procedure 2</p> <p>Increasing Absorbance with increasing sample no.</p>	 <p>Absorption Curve Procedure 1</p> <p>Increasing Absorbance with increasing sample no.</p>

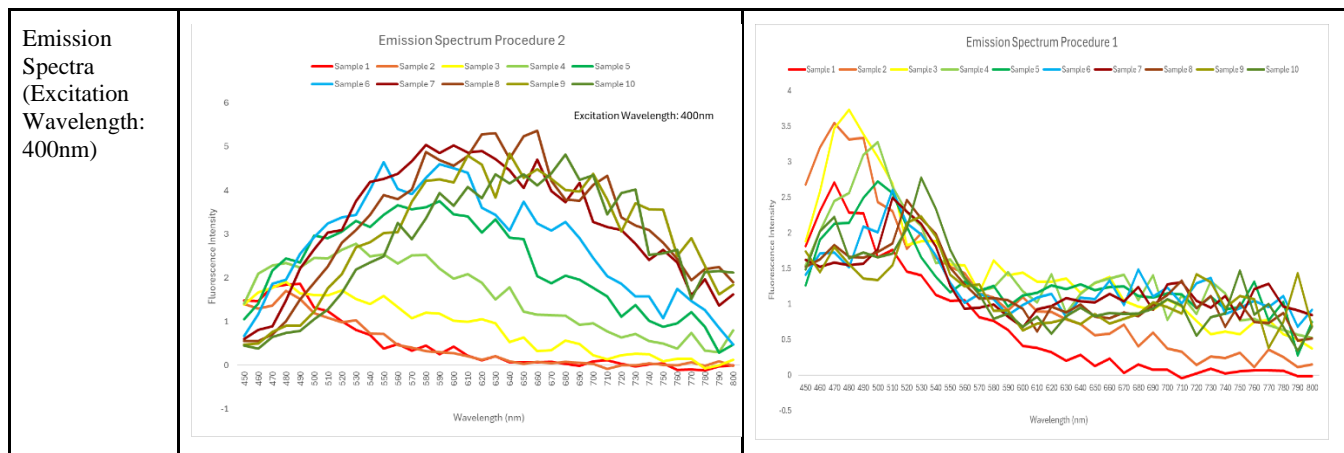


Figure 3: Table showing images of the QD solutions under ambient and UV light as well as their absorption and emission spectra.

With the enhanced particle-in-a-box sphere model, we can calculate the radius (r) with the equation $r = \sqrt{\frac{h^2(\frac{1}{m_e} + \frac{1}{m_h})}{8(\frac{hc}{\lambda} - E_{gap})}}$. With an emission wavelength $\lambda = 400$ nm, we get a radius of $r = 1.66 \times 10^{-9}m = 1.66nm$. Assuming perfectly spherical QDs, we can find the volume, $V = \frac{4\pi r^3}{3} = 1.91 \times 10^{-30}m^3$. With a density of $5.81g/cm^3$ or $5810000g/m^3$ we can find the mass of an individual QD, $m = 5810000 \times 1.91 \times 10^{-30} = 1.11 \times 10^{-25}g$ or $1.11 \times 10^{-28}kg$.

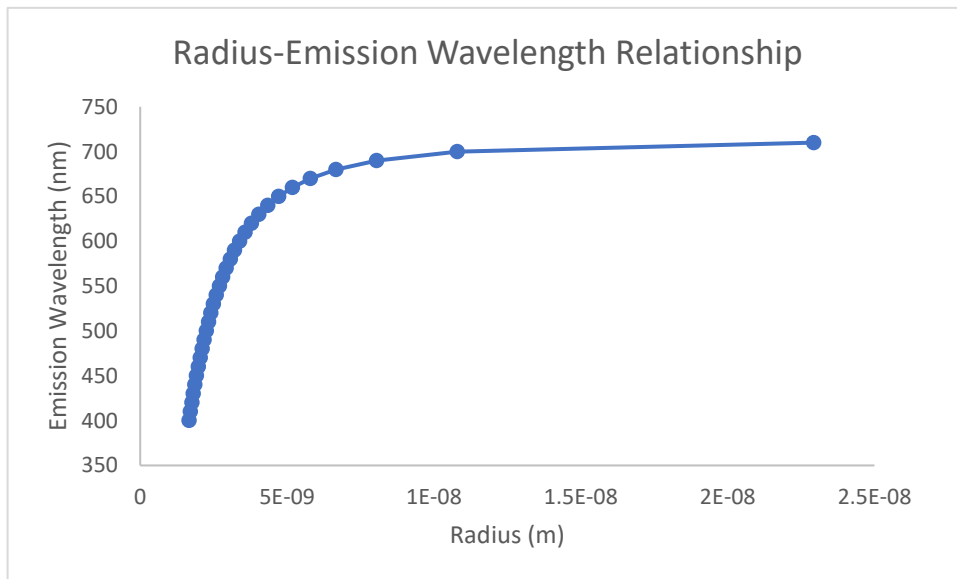


Figure 4: Graph plotting Emission Wavelengths(400-710nm) against the radius of an individual QD.

DISCUSSION: For AuNR synthesis, we observe an initial increase in absorbance values at the start of the experiment in Figure 1 due to the growth of Au nuclei in solution. Au nanoparticles exhibit localised surface plasmon resonance where incident light interacts with surface electrons in the conduction band of the metal, resulting in a shift of absorbance of certain wavelengths. This tends to occur with nanorods with dimensions smaller than the wavelength of incident light (Petrayeva and Krull, 2011, p. 8). With a larger size, more light would interact with the electrons in the conduction band and thus a greater absorbance would be observed.

The surfactant types differ in chain length. CTAB has 16 carbons while C14TAB is shorter with 14 carbons. Adsorption of surfactant molecules on the surface of Au nanorods suggest that the longer surfactant CTAB would protect the longer axis of the nanorod from Au^{3+} deposition better than the shorter C14TAB since there would be more atoms (steric bulk) interfering between the nanorods and free Au^{3+} . Gao et al. also claim that longer chain surfactants led to a greater inhibition of growth of AuNRs on the long axis (2003, p. 9069) which could explain our results. Gao also mentioned that more Au spheres formed instead of nanorods for shorter surfactant molecules such as C10TAB. This indicates that both the concentration and length of the surfactant molecular chain affects the aspect ratio of AuNRs.

From Figure 2, we notice a redshift in the peak absorbance wavelength in the longitudinal mode as the aspect ratio of AuNRs in solution increases. This is due to a phenomenon called surface plasmon resonance (SPR). Electrons in surface atoms exhibit some wave properties and can interact with electromagnetic waves like photons. This could cause the electrons to absorb some energy from photons and begin to oscillate, which we call plasmons (Nguyen et al, 2015). Nanorods have two modes of plasmon resonance, transverse and longitudinal due to its ellipsoidal shape. The transverse and longitudinal modes refer to plasmons oscillating along the shorter width and longer length of the nanorod respectively. As aspect ratio increases, the longitudinal mode tends to oscillate at longer wavelengths due to the increasing length of the nanorod and would more likely interact and absorb energy from longer wavelengths of light. This explains why the peak longitudinal wavelength of light correlates to the aspect ratio of the nanorods as supported by the Brioude equation.

The appearance of the AuNR solutions with longer nanorods however, appear redder than solutions with shorter nanorods, which tend to appear bluer. Figure 2 indicates that more light is absorbed at longer red wavelengths than shorter wavelengths for longer nanorods which seems counterintuitive to our visual observations. If a sample were to absorb more red light, we should observe less red colour since fewer of those photons would enter our eyes. This could be explained by how absorbance is calculated by the spectrometer. Absorbance(A) is related to transmitted(I) and incident light(I_0) by the equation: $A = -\log(I/I_0)$ (Sigma Aldrich, 2024). This means that reflected light off the sample would also contribute to the absorbance value. This suggests that the absorbance values we plotted in Figures 1 and 2 includes light that has been both absorbed and reflected off the sample. The actual appearance of the sample colour could be attributed by the repeated rise and fall in conduction band electron's energy level. When it absorbs light of a certain wavelength and energy, the electron rises to a higher energy level. The electron can then fall back to its resting state, releasing the energy it absorbed as a photon. This photon would then be what we observe as the colour of the solution. Perhaps with an emission spectra, this would be more apparent and we would see less absorbance at longer wavelength for solutions with shorter AuNRs and vice versa for longer AuNRs.

In CdSe QD synthesis, we observed a visible redshift in the solution colour with increasing reaction time. This could be explained by using the particle in a box model to model the electrons in surface atoms. Electrons in semiconductors have discrete energy levels. As a QD increases in radius, the band gap between the conduction and valence bands decreases, resulting in a lower energy, higher wavelength photon to be absorbed and emitted. Giansante and Infante claim that some discontinuities and imperfections in the CdSe crystal lattice could result in unpaired electrons on the surface, allowing the QD to interact with the environment. This could shift the energy levels of the electrons in the lattice and thus cause energy levels between the band gap called trap states to arise (2017, p. 5211). Due to this, an electron may undergo

a fall in energy level to the trap state before reaching its resting state. This results in a lower energy, higher wavelength photon being emitted with larger QDs.

Figure 3 compares the appearance of the QD samples with and without oleylamine under ambient and UV light as well as their corresponding absorption and emission spectra. We observe that the solutions with oleylamine are not as vivid in colour under UV light compared to those without oleylamine. The absorption spectra indicates that as reaction time increases, the absorbance across all wavelengths increases. This could be due to the increasing average radius of QDs in solution, making it more opaque. We also notice the absorption peak wavelengths after 450nm are more redshifted in solutions with oleylamine which is consistent with the literature (Landry et al., 2013, p. 276). Landry et al also suggested that oleylamine may alter surface properties on QDs which results in less trap state emissions which are more intense than exciton emission. This could explain the reduced vividness of colour in the vials with oleylamine and the lower fluorescence intensity values in Procedure 1 compared to in Procedure 2 emission spectra. It is apparent that the emission spectra for Procedure 2 without oleylamine is significantly broader than that of Procedure 1 with oleylamine. Landry et al suggest that this broadness is due to trap state emission. The narrower peaks in Procedure 1 would then result from the reduction of these trap states.

Figure 4 indicates that the greater the radius of a QD, the longer the emission wavelength. This is consistent with the particle in a box model where an increasing QD radius introduces more energy levels and thus a reduced band gap. A smaller band gap implies lower energy photon emission when an electron drops from the conduction to the valence band. This is why larger QDs appear redder and vice versa. From the shape of the curve, we can see that the radius of QDs do not grow linearly but resembles logarithmic growth.

CONCLUSION: We have explored AuNR synthesis, and the effect of surfactant type (length) has on the aspect ratio as well as CdSe Quantum Dot synthesis. Longer chain surfactants are more effective in increasing the AuNR aspect ratio due to a greater degree of steric hindrance in AuNR synthesis. In QD synthesis, we discovered that Oleylamine could reduce trap state emission, resulting in narrower emission spectrum peaks, with the downside of reduced fluorescence intensity. These experiments have highlighted the surface properties of these nanoparticles where a small change in size leads to a significant macroscopic change in colour.

AUTHOR INFORMATION

Corresponding Author

Email: felix.syn22@imperial.ac.uk

Author Contributions

The manuscript was written through contributions of all authors.

Funding Sources

Department of Bioengineering, Imperial College London

ACKNOWLEDGMENT

The author acknowledges the contributions of Hu Changyu and Danil Zadorozhnyi in carrying out the experiments stated in this paper.

ABBREVIATIONS

AuNR, Gold Nanorods; CdSe, Cadmium Selenide; QD, Quantum Dots.

REFERENCES

1. Brioude, A., Jiang, X.C., Pileni, M.P., 2005. Optical Properties of Gold Nanorods: DDA Simulations Supported by Experiments. *The Journal of Physical Chemistry B* 109, 13138–13142. <https://doi.org/10.1021/jp0507288>
2. Gao, J., Bender, C.M., Murphy, C.J., 2003. Dependence of the Gold Nanorod Aspect Ratio on the Nature of the Directing Surfactant in Aqueous Solution. *Langmuir* 19, 9065–9070. <https://doi.org/10.1021/la034919i>
3. Giansante, C., Infante, I., 2017. Surface Traps in Colloidal Quantum Dots: A Combined Experimental and Theoretical Perspective. *The Journal of Physical Chemistry Letters* 8, 5209–5215. <https://doi.org/10.1021/acs.jpclett.7b02193>
4. Landry, M.L., Morrell, T.E., Karagounis, T.K., Hsia, C.-H., Wang, C.-Y., 2013. Simple Syntheses of CdSe Quantum Dots. *Journal of Chemical Education* 91, 274–279. <https://doi.org/10.1021/ed300568e>
5. Mosquera, J., Wang, D., Bals, S., Liz-Marzán, L.M., 2023. Surfactant Layers on Gold Nanorods. *Accounts of Chemical Research* 56, 1204–1212. <https://doi.org/10.1021/acs.accounts.3c00101>
6. Petryayeva, E., Krull, U.J., 2011. Localized surface plasmon resonance: Nanostructures, bioassays and biosensing—A review. *Analytica Chimica Acta* 706, 8–24. <https://doi.org/10.1016/j.aca.2011.08.020>
7. Nguyen, H., Park, J., Kang, S., Kim, M., 2015. Surface Plasmon Resonance: A Versatile Technique for Biosensor Applications. *Sensors* 15, 10481–10510. <https://doi.org/10.3390/s150510481>
8. Sigma Aldrich, 2024. Transmittance to Absorbance Table [WWW Document]. URL <https://www.sigmaaldrich.com/GB/en/technical-documents/technical-article/analytical-chemistry/photometry-and-reflectometry/transmittance-to-absorbance> (accessed 1.26.24).